P2Y6 receptor mediates colonic NaCl secretion via differential activation of cAMP-mediated transport

Michael Köttgen,[1] Thomas Löffler,[2] Christoph Jacobi,[2] Roland Nitschke,[2] Hermann Pavenstädt,[3] Rainer Schreiber,[2] Sebastian Frische,[3] Søren Nielsen,[3] and Jens Leipziger[4]

[1]Medizinische Universitätsklinik, Freiburg, Germany
[2]Physiologisches Institut, Albert-Ludwigs-Universität, Freiburg, Germany
[3]Institute of Anatomy, and
[4]Institute of Physiology, The Water and Salt Research Center, Aarhus University, Aarhus C, Denmark

Extracellular nucleotides are important regulators of epithelial ion transport. Here we investigated nucleotide-mediated effects on colonic NaCl secretion and the signal transduction mechanisms involved. Basolateral UDP induced a sustained activation of Cl^- secretion, which was completely inhibited by 293B, a specific inhibitor of cAMP-stimulated basolateral KCNQ1/KCNE3 K^+ channels. We therefore speculated that a basolateral $P2Y_6$ receptor could increase cAMP. Indeed UDP elevated cAMP in isolated crypts. We identified an epithelial $P2Y_6$ receptor using crypt $[Ca^{2+}]_i$ measurements, RT-PCR, and immunohistochemistry. To investigate whether the rat $P2Y_6$ elevates cAMP, we coexpressed the $P2Y_1$ or $P2Y_6$ receptor together with the cAMP-regulated cystic fibrosis transmembrane conductance regulator (CFTR) Cl^- channel in *Xenopus* oocytes. A two-electrode voltage clamp was used to monitor nucleotide-induced Cl^- currents. In oocytes expressing the $P2Y_1$ receptor, ATP transiently activated the endogenous Ca^{2+}-activated Cl^- current, but not CFTR. In contrast, in oocytes expressing the $P2Y_6$ receptor, UDP transiently activated the Ca^{2+}-activated Cl^- current and subsequently CFTR. CFTR Cl^- currents were identified by their halide conductance sequence. In summary we find a basolateral $P2Y_6$ receptor in colonic epithelial cells stimulating sustained NaCl secretion by way of a synergistic increase of $[Ca^{2+}]_i$ and cAMP. In support of these data $P2Y_6$ receptor stimulation differentially activates CFTR in *Xenopus* oocytes.

J. Clin. Invest. **111**:371–379 (2003). doi:10.1172/JCI200316711.

Introduction

Nucleotides are ubiquitous extracellular signaling molecules that induce a wide spectrum of biological responses (1). The cellular effects of extracellular nucleotides are mediated by P2 receptors, which are subdivided into two families, P2X and P2Y receptors (2). P2X receptors are ATP-gated ion channels, whereas P2Y receptors belong to the superfamily of G protein–coupled receptors (2). The mammalian P2Y family includes the $P2Y_1$, $P2Y_2$, $P2Y_4$, $P2Y_6$, $P2Y_{11}$, $P2Y_{12}$, and $P2Y_{13}$ receptor (2–4). The P2Y receptor subtypes differ pharmacologically in their selectivity for adenine and uracil nucleotides (2).

Received for publication August 20, 2002, and accepted in revised form December 4, 2002.

Address correspondence to: Jens Leipziger, Institute of Physiology, The Water and Salt Research Center, Aarhus University, Ole Worms Allé 160, 8000 Aarhus C, Denmark. Phone: 0045-89422826; Fax: 0045-86129065; E-mail: leip@fi.au.dk.

Conflict of interest: The authors have declared that no conflict of interest exists.

Nonstandard abbreviations used: cystic fibrosis transmembrane conductance regulator (CFTR); transepithelial voltage (V_{te}); transepithelial resistance (R_{te}); voltage deflections (ΔV_{te}); short circuit current (I_{sc}); 3-isobutyl-1-methylxanthine (IBMX); *trans*-6-cyano-4-(*N*-ethylsulphonyl-*N*-methylamino)-3-hydroxy-2,2-dimethyl-chromane (293B); tetrodotoxin (TTX).

P2Y receptors are found in a variety of epithelial tissues and are shown to function as important regulators of ion transport (5–8).

Electrolyte transport of the mammalian colon involves both absorptive and secretory processes. Transport is characterized by absorption of NaCl, K^+, H_2O, and short-chain fatty acids (9, 10). NaCl is either absorbed electroneutrally by parallel apical Cl^-/HCO_3^- and Na^+/H^+ antiporters or electrogenically by apical ENaC channels located in the distal colon (10). In addition, the colon is able to secrete NaCl, K^+, HCO_3^-, and mucous (10). In some diseases, such as colitis ulcerosa, an increased secretion is thought to be involved in the pathogenesis of diarrhea (10). Absorption is confined predominantly to surface enterocytes, whereas secretion is most pronounced in crypt cells (9). Colonic NaCl secretion follows the general scheme of nearly all secretory glands in the gastrointestinal tract and other organ systems (Figure 1a) (11). Cl^- is transported transcellularly. Cl^- uptake occurs via a basolateral $Na^+/2Cl^-/K^+$ cotransporter. Luminal Cl^- exit occurs via cystic fibrosis transmembrane conductance regulator (CFTR) Cl^- channels, which are activated by cAMP (12). NaCl secretion requires basolateral K^+ channels providing the necessary driving force for luminal Cl^- exit. The cAMP-activated KCNQ1/KCNE3 K^+ channels and intermediate conductance Ca^{2+}-activated SK4 channels have been

shown to drive secretion (13–15). A typical secretory agonist such as PGE_2 elevates cAMP, which activates luminal CFTR and basolateral KCNQ1/KCNE3 channels (11). In contrast, activation of muscarinic receptors increases $[Ca^{2+}]_i$ and activates SK4 channels to elevate the driving force for Cl^- exit (13). Parallel activation of both pathways dramatically increases secretion (16).

Recent work has highlighted a significant regulation of colonic ion transport via luminal and basolateral P2 receptors. These include luminal P2Y receptor–mediated activation of K^+ secretion and inhibition of electrogenic Na^+ absorption (17, 18). Furthermore, basolateral $P2Y_1$ receptor stimulation transiently activates NaCl secretion (6).

This study identifies a basolateral epithelial $P2Y_6$ receptor mediating sustained NaCl secretion. In contrast to the $P2Y_1$ receptor, stimulation of the $P2Y_6$ receptor leads to an increase in $[Ca^{2+}]_i$ and cAMP, which synergistically activates NaCl secretion.

Methods

Ussing chamber experiments. Ussing chamber experiments were performed as described previously (17). Briefly, the muscle layer of rat (70–120 g) distal colon was removed, and the mucosa was mounted in an Ussing chamber. The measurements were performed in "open-circuit" mode. Transepithelial voltage (V_{te}) was referred to the serosal side. Transepithelial resistance (R_{te}) was calculated from the voltage deflections (ΔV_{te}) induced by short current pulses every 3 seconds (25 μA, 0.6 sec) (19). The equivalent short circuit current (I_{sc}) — a measure of electrogenic ion transport — was obtained by Ohm's law from V_{te}/R_{te}. The calculated I_{sc} changes were derived from peak values.

Digital video imaging of $[Ca^{2+}]_i$. The preparation and handling of colonic crypts was performed as described formerly (6, 20). An inverted microscope (Axiovert 100 TV; Carl Zeiss Jena GmbH, Jena, Germany) with a ×40 objective (Fluar ×40, 1.3 oil; Carl Zeiss Jena GmbH), a monochromator (Till Photonics GmbH, Martinsried, Germany), and a digital camera (Micromax 5 MHz; Princeton Instruments Inc., Trenton, New Jersey, USA) were used. Image acquisition and data analysis were performed with the software package Metamorph/Metafluor (Universal Imaging Corp., West Chester, Pennsylvania, USA). Crypts were incubated in 10 μM fura-2/AM for 10 minutes at room temperature in Ringer's solution to which 1.6 μM pluronic F127 and 5 mM probenecid had been added. Experiments were performed with the following bath solution (in millimoles per liter): 145 NaCl, 1 $MgCl_2$, 1.3 Ca-gluconate, 5 D-glucose, 0.4 KH_2PO_4, 1.6 K_2HPO_4. All solutions had a pH of 7.4. As a measure of $[Ca^{2+}]_i$, the fluorescence emission ratio at 345 nm/380 nm excitation was calculated. The fluorescence signal was recorded from the base and the middle part of the crypt.

Measurement of intracellular cAMP. For each experiment all collected crypts from 2 cm of distal colon from two rats were used. Colonic crypts were isolated as described and divided into different groups. Each group was composed of six samples of crypt suspension. All experiments were performed with 3-isobutyl-1-methylxanthine (IBMX; 100 μM). Each group of colonic crypts was exposed to the added agents as indicated for 3 minutes. To terminate the assay, the supernatants were rapidly removed, and crypts were rinsed with ice-cold ethanol (70%). After ethanol extraction, cAMP concentrations were measured with an ELISA (Amersham Buchler, Braunschweig, Germany). Because the absolute number of crypts analyzed could be variable between experiments, we first calculated the mean cAMP concentration of the control for each experiment. The measured values of the other conditions were standardized to the mean control concentration of the corresponding experimental group and expressed as the percentage of change.

Cloning of the $P2Y_1$ and $P2Y_6$ receptor from isolated rat colonic crypts. Total RNA was extracted from approximately 500 isolated colonic crypts using QuickPrep Micro mRNA Purification Kit (Pharmacia Diagnostics GmbH, Freiburg, Germany). Total RNA was transcribed into cDNA using RT-PCR (Life Sciences Inc., Berlin, Germany) and DNA-polymerase (TurboPfu; Stratagene Europe, Amsterdam, the Netherlands). A homology strategy was applied, using primers based on published sequences from either rat insulinoma cells (21) (sense: 5′ GCCTGAGTTGGAAAGAAGAG 3′; antisense: 5′ GCTTGGATCTCCTGCCTTC 3′) ($P2Y_1$) and rat aortic smooth muscle cells (22) ($P2Y_6$) (sense: 5′ CGCCAGCCATGGAGCGGG 3′; antisense: 5′ GGTCTCAGACTCTCTGCCTC 3′). Sequencing of the amplified receptor DNA was carried out using the thermo-Sequenase II dye terminator cycle sequence kit (kit no. 79765; Amersham Buchler) and an Applied Biosystems Inc. 373A DNA Sequencer (Foster City, California, USA).

Generation of an Ab against rat $P2Y_6$ receptors and immunohistochemistry. A polyclonal peptide Ab from rabbit against the C-terminal end of the rat $P2Y_6$ receptor was generated (Davids Biotechnologie, Regensburg, Germany). As an epitope we chose the C-terminal end from amino acid 282–298. Rat colon was fixed by retrograde perfusion via the aorta with 4% paraformaldehyde in 0.1 M cacodylate buffer pH 7.4 and postfixed for 2 hours in similar fixative. Colon slices were dehydrated and embedded in paraffin. The paraffin-embedded tissue was cut at 2 μm on a rotary microtome (Leica Mikrosysteme, Bensheim, Germany). The sections were dewaxed and rehydrated. To reveal antigens, sections were placed in 10 mM Tris buffer (pH 9.0) supplemented with 0.5 mM EGTA and were heated using a microwave oven for 10 minutes. Nonspecific binding of immunoglobulin was prevented by incubating the sections in 50 mM NH_4Cl for 30 minutes followed by blocking in PBS supplemented with 1% BSA, 0.05% saponin, and 0.2% gelatin. Sections were incubated overnight at 4°C with $rP2Y_6$ Ab's diluted 1:10,000 in 10 mM PBS, pH 7.4, containing 0.1% Triton X-100 and 0.1% BSA. Subsequently, sections were incubated with horseradish peroxidase–

linked goat anti-rabbit secondary Ab's (P448; DAKO A/S, Glostrup, Denmark), and 3,3-diaminobenzidine technique was used to visualize the labeling. Finally the sections were counterstained using Mayer's hematoxylin. Absorption controls were performed by incubating the Ab's with matrix-bound immunizing peptide for 4 hours prior to labeling of the sections, using the supernatant at similar dilution as the untreated Ab's. Preimmune serum and serum from another rabbit was applied at 1:10,000 dilution.

Preparation and injection of oocytes. Xenopus oocytes (H. Kähler, Bedarf für Entwicklungsbiologie, Hamburg, Germany) were isolated and injected as described previously (23). Briefly, 12–24 hours following isolation, healthy-looking stage V–VI oocytes were injected with 30 nl of water containing either 10 ng cRNA of rat $P2Y_1$, $P2Y_6$, or human wild-type CFTR. In coexpressing oocytes, we initially injected human wild-type CFTR followed by the respective purino receptor cRNA 24–48 hours later. Voltage clamp experiments were performed 2 to 5 days after injection.

Two-electrode voltage clamp. Whole cell currents of oocytes were recorded using the World Precision Instruments oocyte clamp amplifier (OOC-1; Berlin, Germany). Microelectrodes were pulled on a vertical puller (Physiologisches Institut, Universität Freiburg, Freiburg, Germany) from borosilicate glass capillaries (Clark Instruments, Reading, United Kingdom) and had resistance of 0.5–2 MΩ when filled with 2 M KCl solution. Experiments were performed at 20–22°C. All whole-cell voltage-clamp experiments were conducted in ND96 solution (96 mM NaCl, 2 mM KCl, 1.8 mM $CaCl_2$, 1 mM $MgCl_2$, 5 mM HEPES, 2.5 mM Na-pyruvate, pH 7.4). The voltage-clamp protocol was –30, –80, –40, +60 mV (each step 1 second). Whole-cell conductance was calculated according to Ohm's law. Water-injected or noninjected oocytes had slope conductance smaller than 4 μS when clamped ± 20 mV from their membrane voltage (close to –30 mV).

Confocal microscopy. The voltage-clamp system was adapted to an inverted confocal microscope (LSM510; Carl Zeiss Jena GmbH) equipped with a ×10 objective (Plan-Neofluar ×10/0.3; Carl Zeiss Jena GmbH). $[Ca^{2+}]_i$ changes were measured with Oregon Green Bapta-1. Twenty-four hours after the measurement, purino receptor-expressing oocytes were injected with 25 nl Oregon Green Bapta-1 (1 mM, dissolved in intracellular Ringer type solution containing 95 mM K gluconate, 30 mM KCl, 1.2 mM NaH_2PO_4, 4.8 mM Na_2HPO_4, 5 mM glucose, 1 mM $MgCl_2$, 0.5 M EGTA, pH 7.2), yielding an approximate oocyte dye concentration of 20 μM. After mounting and impalement of the oocytes, the simultaneous measurement of whole-cell current and $[Ca^{2+}]_i$ was started. Oregon Green Bapta-1 was excited at 488 nm with a blue-enhanced argon laser, and its emission was collected at more than 500 nm from horizontal *xy* scans across the animal pole facing toward the bath bottom and objective lens. Sequential images were analyzed by measuring mean pixel intensity versus time in individual oocytes.

Solutions and chemicals. Pluronic F127, LY, and fura-2/AM were obtained from Molecular Probes Inc. (Eugene, Oregon, USA). Collagenase was obtained from Worthington Biochemical (Lakewood, New Jersey, USA). IBMX and all other chemicals were of the highest grade of purity available and were obtained from Sigma-Aldrich (Deisenhofen, Germany) and Merck KGaA (Darmstadt, Germany). The 293B (trans-6-cyano-4-(*N*-ethylsulphonyl-*N*-methylamino)-3-hydroxy-2,2-dimethyl-chromane) was provided by Aventis Pharma AG (Frankfurt am Main Frankfurt, Germany). Commercially available nucleotide diphosphates are frequently contaminated with nucleotide triphosphates. To circumvent this problem we treated the ADP and UDP stock solution as described by Nicholas et al. for 1 hour in 10 U/ml hexokinase and 22 mM glucose, which was shown to result in the complete conversion of UTP to UDP and ATP to ADP (24).

Statistics. The data are shown as mean values ± SEM (*n*), where *n* refers to the number of experiments. The paired or unpaired *t* test was used to compare mean values within one or different experimental series. A *P* value less than 0.05 indicated statistical significance.

Results

Basolateral UDP activates a persistent Cl^- secretion in rat distal colonic mucosa. In a previous study we presented evidence for the functional expression of a basolateral $P2Y_1$ receptor in rat distal colonic mucosa, which stimulates NaCl secretion by an increase of cytosolic calcium (6). Here we extend these studies to investigate the functional expression of additional P2Y receptors in the basolateral membrane of rat colonic epithelium. A typical example of an Ussing chamber experiment — performed to study the effects of nucleotides on colonic ion transport — is depicted in Figure 1b. Before addition of nucleotides, the mucosa was treated with 10 μM luminal amiloride to inhibit electrogenic Na^+ reabsorption. Additionally, basolateral tetrodotoxin (TTX) (1 μM) was applied to reduce effects due to neuronal activation of ion transport. This treatment with amiloride and TTX substantially reduced V_{te} and increased R_{te}, reflecting a significant reduction of electrogenic ion transport. Subsequently, ATP (1 mM) was added to the basolateral side, leading to a transient deflection of V_{te}. During ATP stimulation, R_{te} decreased (6).

We now investigated the effect of basolateral UDP as a specific agonist of $P2Y_6$ receptors. Like ATP, UDP increased the lumen-negative V_{te} and simultaneously reduced R_{te} if added from the basolateral side. Luminal UDP was without effect ($n = 7$). An important difference between the "secretory" response of the two nucleotides is obvious when comparing Figure 1, b and c. Whereas the effect of ATP was transient, that of UDP showed a persistent activation of secretion. Furthermore, the effect of UDP was completely inhibited by 293B, a specific inhibitor of the KCNQ1/KCNE3 K^+

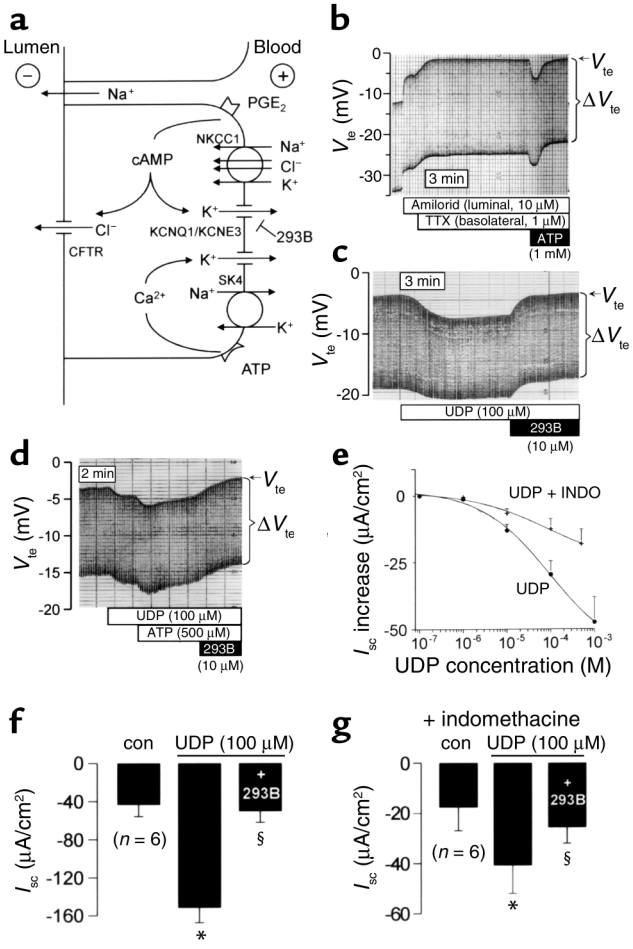

Figure 1
Effects of ATP and UDP on colonic ion transport. (**a**) Model of NaCl secretion in colonic enterocyte. (**b**) Original recording of transepithelial voltage (V_{te}) and transepithelial voltage changes (ΔV_{te}). The upper line shows V_{te} and the bandwidth of voltage deflections reflects the transepithelial resistance (R_{te}, see Methods). Application of ATP to the basolateral side led to a transient deflection of V_{te}, and decreased R_{te}. (**c**) Basolateral UDP increased the lumen-negative V_{te} and decreased R_{te} persistently. This effect was completely blocked by 293B. (**d**) Additive effect of basolateral UDP and ATP. (**e**) Concentration response curve of UDP in the presence (+) and absence (filled circles) of indomethacin (50 μM). The equivalent short circuit current (I_{sc}) was calculated according to Ohm's law (see Methods). (**f**) Effect of 293B (10 μM) on the UDP-induced increase of I_{sc} in the absence and presence (**g**) of indomethacin (* and § indicate significant changes). Con, control.

channels (25), whereas the ATP-mediated response was insensitive to 293B (data not shown; n = 5). In rat colonic mucosa this K^+ channel is activated by cAMP and provides the driving force for CFTR-mediated Cl^- extrusion across the apical membrane (14, 19). Surprisingly, the effect of UDP resembles that of other colonic secretory agonists such as vasointestinal peptide or adenosine, which mediate their effect by elevating cAMP (10). A number of $[Ca^{2+}]_i$–elevating agonists have been shown to mediate NaCl secretion in gut and other secretory tissues indirectly by activation of PGE_2 production, which subsequently increases cAMP (26, 27). We therefore inhibited PGE_2 production with indomethacin (50 μM) 30 minutes before adding UDP. Figure 1e shows the concentration response curve of basolateral UDP in the absence (EC_{50}: 90 μM) and presence of indomethacin (EC_{50}: 85 μM). The UDP-mediated secretory response was substantially reduced in the presence of indomethacin. Figure 1, f and g, summarizes the series of experiments. Without indomethacin, UDP (100 μM) increased I_{sc} from a resting value of –43.2 ± 12.7 to –151.9 ± 15.8 μA/cm². Addition of 293B (10 μM) completely inhibited the UDP-induced I_{sc} to –50.1 ± 11.9 μA/cm² (n = 6). In the presence of indomethacin, resting I_{sc} amounted to –17.6 ± 9.3 and increased with UDP (100 μM) to –40.6 ± 11.3 μA/cm². Again, 293B (10 μM) completely inhibited the UDP-stimulated secretion to –25.5 ± 6.4 μA/cm² (n = 6).

Furthermore, we demonstrated additivity of ADP- and UDP-stimulated (100 μM) Cl^- secretion; I_{sc} increases UDP alone: 32.8 ± 9.54 μA/cm². Subsequent addition of ADP increased I_{sc} further by 18.9 ± 5.2 μA/cm² (n = 5). Similar results were obtained when UDP (100 μM) and ATP (500 μM) were added (n = 6). An original experiment is shown in Figure 1d.

From these results we derived the following hypotheses: (a) In addition to the previously described expression of a basolateral $P2Y_1$ receptor, rat colonic crypt cells also express a basolateral UDP-sensitive $P2Y_6$ receptor. (b) Activation of this receptor mediates sustained NaCl secretion. (c) This $P2Y_6$ receptor-activated secretion is mediated by a synergistic increase of $[Ca^{2+}]_i$ and cAMP.

UDP increases cytosolic Ca^{2+} in colonic crypts. Subsequently, we investigated whether the effect of UDP on colonic ion transport was mediated by receptors expressed in colonic enterocytes. We therefore performed measurements of $[Ca^{2+}]_i$ in intact colonic crypts. In Figure 2, a and b, it is shown that both UDP (100 μM) and ATP (100 μM) significantly increase $[Ca^{2+}]_i$. UDP reversibly increased the fura-2 fluorescence ratio (345 nm/380 nm) from 1.15 ± 0.04 to 1.23 ± 0.04 (n = 23). ATP reversibly elevated the fura-2 ratio from 1.16 ± 0.04 to a peak value of 1.82 ± 0.12 (n = 23).

Measurement of cAMP in rat colonic crypts. Furthermore, we measured resting and stimulated cAMP concentrations in isolated rat colonic crypts. The data are summarized in Figure 2c. As positive controls we used PGE_2 and forskolin, agonists known to increase cAMP in colonic enterocytes (28). Concentrations of cAMP were significantly increased to 140% ± 5%, 151% ± 15%, and 2,149% ± 13% by UDP, PGE_2, and forskolin, respectively. The small ATP-mediated cAMP increase was not significant.

Immunohistochemical localization of $P2Y_6$ receptor in rat colonic mucosa. Figure 3a shows the immunohistochemical localization of rat $P2Y_6$ receptors in distal rat colonic mucosa. Clearly, the $rP2Y_6$ Ab's label the mucosal epithelium and singular submucosal cells.

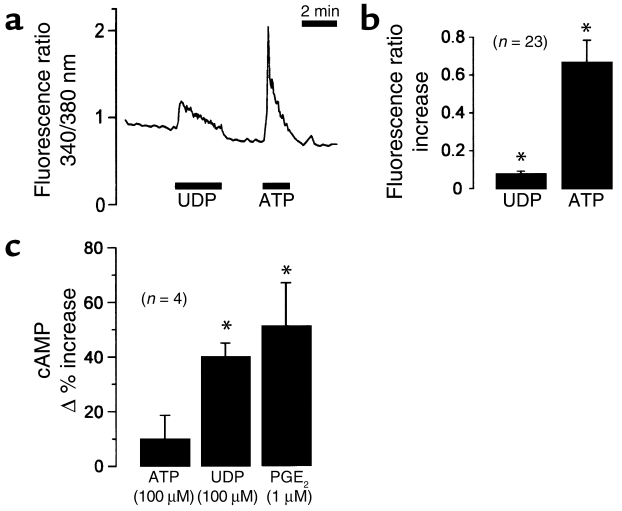

Figure 2
(**a**) Original recording of fura-2 fluorescence ratio measurement in an isolated colonic crypt. Both UDP (100 μM) and ADP (100 μM) in the bath solution lead to an increase in $[Ca^{2+}]_i$. (**b**) Summary of UDP-induced (100 μM) and ADP-induced effects on cytosolic Ca^{2+} in isolated colonic crypts. *Significant change induced by ATP or UDP. (**c**) Effect of different agonists on the production of cAMP. All experiments were performed in the presence of IBMX (0.1 mM). *Significant difference from control ($P > 0.05$).

Upon incubation with rabbit serum, singular submucosal cells were labeled, indicating unspecific binding of IgG in these cells (insert in Figure 3a). Specific mucosal staining of the $rP2Y_6$ receptor is further strengthened by basolateral staining in rat proximal tubule (S1 to S2) by the same Ab, a tissue recently described to express the $P2Y_6$ receptor (our unpublished observations) (29).

Cloning of the $P2Y_1$ and $P2Y_6$ receptor from rat colonic crypts. Based on the pharmacological data presented above, we postulated the expression of basolateral $P2Y_1$ and $P2Y_6$ receptors in epithelial cells of rat colon. RT-PCR experiments with cDNA from colonic crypt cells indicated the expression of the two receptors (data not shown). We subsequently cloned the two receptors from cDNA of colonic crypt cells using primers based on the published sequences (see Methods). The PCR products for the $P2Y_1$ and $P2Y_6$ receptor had the expected length of 1,160 and 999 bp, respectively. Sequencing of the cloned $P2Y_1$ and $P2Y_6$ receptor confirmed identity to the above-mentioned and published sequences (data not shown).

Heterologous expression of the rat $P2Y_1$ and $P2Y_6$ receptor in Xenopus oocytes. The unexpected observation that UDP led to an apparent activation of cAMP-stimulated secretion in rat colonic mucosa prompted us to study the signal transduction mechanisms of the $P2Y_1$ and $P2Y_6$ receptor in more detail. To this end we expressed the cloned receptors in *Xenopus* oocytes, which do not express endogenous P2Y receptors. Functional expression of $P2Y_1$ and $P2Y_6$ receptors was shown by combined measurement of cytosolic Ca^{2+} and whole cell current. Activation of both receptors led to a rise in $[Ca^{2+}]_i$. This rise in $[Ca^{2+}]_i$ induced a parallel increase in whole-cell current due to activation of Ca^{2+}-activated Cl^- channels in $P2Y_1$ and $P2Y_6$ receptor–expressing oocytes (Figure 4; $n = 5$ and $n = 3$). It is evident that the Ca^{2+}-activated Cl^- conductance of the oocytes closely reflects the $[Ca^{2+}]_i$ increase. Application of nucleotides to water-injected oocytes neither had an effect on cytosolic Ca^{2+} nor did it affect whole cell conductance ($n = 10$).

We then characterized the effects of ATP and UDP on the whole-cell conductance of P2Y receptor–expressing oocytes. In $P2Y_1$ receptor–expressing oocytes ATP (10 μM) led to a fast and transient increase in whole current (Figure 5a). The calculated whole-cell conductance in these experiments increased from 3.0 ± 0.52 to 63.08 ± 6.79 μS ($n = 12$) at the peak of the conductance increase. The biophysical characterization of the whole-cell conductance revealed an outwardly rectifying current-voltage relationship with a reversal potential near the equilibrium potential for Cl^- (–30 mV; Figure 5c). The halide conductance sequence was $I^- > Br^- > Cl^-$, which is characteristic for the endogenous Ca^{2+}-activated Cl^- conductance of *Xenopus* oocytes (Figure 5, b and d). Likewise, UDP increased the whole cell conductance in $P2Y_6$ receptor–expressing oocytes from

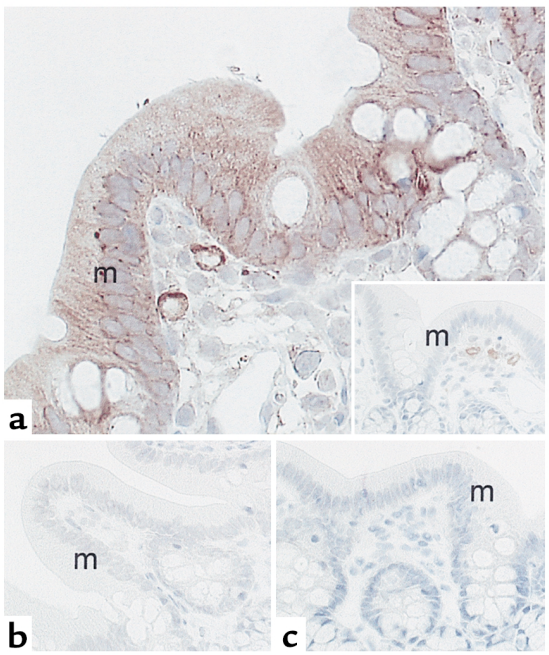

Figure 3
Immunohistochemistry of rat colon. The $rP2Y_6$-Ab's label the mucosal epithelium (m) and singular submucosal cells (**a**). Upon incubation with rabbit serum, singular submucosal cells were labeled, indicating unspecific binding of IgG in these cells (insert in **a**). Incubation with $rP2Y_6$ Ab's, which had been preabsorbed with the immunizing peptide (**b**). Incubation with preimmune serum (**c**).

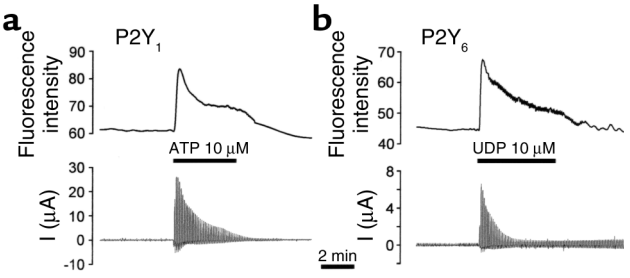

Figure 4
Combined measurement of $[Ca^{2+}]_i$ and whole-cell current in *Xenopus* oocytes. Upper trace: Oregon green fluorescence intensity as a measure of $[Ca^{2+}]_i$. Lower trace: whole-cell current measured with the double-electrode voltage-clamp technique (voltage-clamp protocol: –30, –80, –40, +60 mV for 1 second, respectively). (**a**) ATP induced a parallel increase in $[Ca^{2+}]_i$ and whole-cell current in oocytes expressing the $P2Y_1$ receptor. (**b**) In $P2Y_6$ receptor–expressing oocytes UDP raised $[Ca^{2+}]_i$ and whole-cell current.

4.58 ± 0.43 μS to 54.04 ± 3.34 μS (n = 17; Figure 5e). The current-voltage relationship and the halide conductance sequence were very similar to that of $P2Y_1$-expressing oocytes (Figure 5, f–h).

To test the selectivity of the two receptors for purines versus pyrimdines we applied ATP and UDP (both 10 μM) in $P2Y_1$- or $P2Y_6$-expressing oocytes. These experiments confirmed the published selectivity of ATP > >UDP for the $P2Y_1$ receptor and UDP > >ATP for the $P2Y_6$ receptor (Figure 5, i and j).

Coexpression of P2Y₁ and P2Y₆ receptor with CFTR in Xenopus oocytes. To monitor dynamic changes of the cytosolic cAMP concentration we coexpressed the CFTR together with the respective P2Y receptor. CFTR functions as a Cl^- channel, which is known to be activated by cAMP. The CFTR Cl^- conductance and the Ca^{2+}-activated Cl^- conductance can be distinguished easily by a different current-voltage relationship and an inverse halide conductance sequence.

Figure 6 shows a typical experiment with an oocyte expressing the $P2Y_1$ receptor and CFTR. In these oocytes ATP also induced a fast increase of the endogenous Cl^- conductance with a halide conductance sequence of $I^- > Br^- > Cl^-$ reflecting an increase in $[Ca^{2+}]_i$. The whole-cell conductance increased from 2.94 ± 0.39 μS to 65.04 ± 5.23 μS in the presence of ATP (10 μM, n = 17). When these coexpressing oocytes were treated with IBMX and forskolin (1 mM and 2 μM), they showed an increase in conductance that could not be observed in oocytes that were not injected with CFTR cRNA. In contrast to the Ca^{2+}-activated Cl^- conductance the CFTR Cl^- conductance had a linear current-voltage relationship and a halide conductance sequence of $Cl^- > Br^- > I^-$ (Figure 6). The maximal increase in whole-cell conductance induced by IBMX/forskolin amounted to 55.2 ± 8.2 μS (n = 17).

Stimulation of the P2Y₆ receptor activates CFTR. We now coexpressed the $P2Y_6$ receptor and CFTR in oocytes. Assuming that stimulation of the $P2Y_6$ receptor could possibly increase cAMP, one would expect that UDP should activate CFTR in these oocytes. In fact, UDP not only increased the Ca^{2+}-activated Cl^- conductance, but also led to an activation of CFTR. UDP (10 μM)

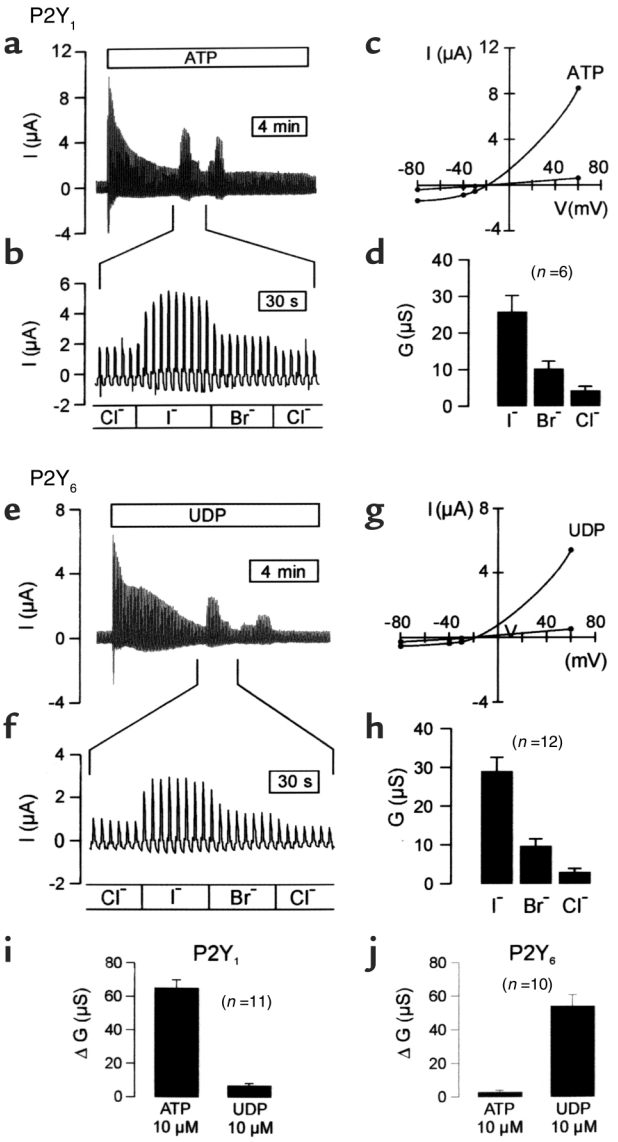

Figure 5
Whole-cell conductive properties of *Xenopus* oocytes expressing the $P2Y_1$ and $P2Y_6$ receptors alone. $P2Y_1$: (**a**) ATP (10 μM) induced a fast increase in whole-cell current (clamp protocol see Figure 4). (**b**) Halide conductance sequence enlarged from **a**. (**c**) Current-voltage relationship of the ATP-induced whole-cell conductance. (**d**) Summary of halide conductance sequence experiments. $P2Y_6$ (**e**) UDP (10 μM) induced a fast increase in whole-cell current (clamp protocol see Figure 4). (**f**) Halide conductance sequence enlarged from **e**. (**g**) Current-voltage relationship of the UDP-induced whole-cell conductance. (**h**) Summary of halide conductance sequence experiments. (**i** and **j**) Nucleotide selectivity of the cloned P2Y receptors. (**i**) Nucleotide-induced conductance increase in $P2Y_1$ receptor–expressing oocytes. (**j**) Nucleotide-induced conductance increase in $P2Y_6$ receptor–expressing oocytes.

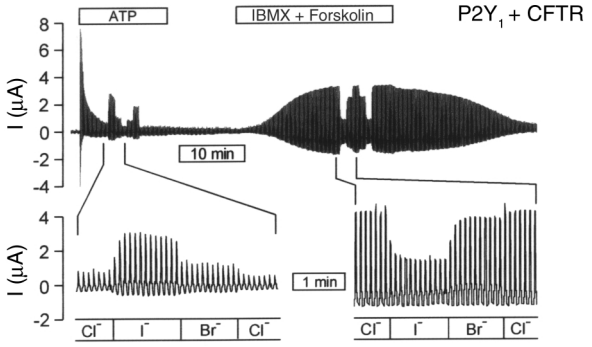

Figure 6
Effect of ATP and IBMX + forskolin on whole-cell conductance in oocytes coexpressing the $P2Y_1$ receptor and CFTR (ATP 10 μM, IBMX 1 mM, forskolin 2 μM). Note the different halide conductance sequence (ATP vs. IBMX + forskolin).

initially led to a fast increase of the outwardly rectifying oocyte Cl^- conductance followed by a slower increase of a conductance with linear current-voltage relationship (Figure 7a). The slower component of the UDP-induced conductance increase reached its maximum after 6.1 ± 0.2 minutes (n = 18). Comparison of the biophysical properties of the Cl^- conductance induced by UDP with the CFTR Cl^- conductance induced by IBMX/forskolin revealed that the halide conductance sequence and the current-voltage relationship were identical (Figure 7, b–e). These data show that the stimulation of the $P2Y_6$ receptor activates both the Ca^{2+}-activated Cl^- conductance and CFTR, a cAMP-regulated Cl^- channel.

Discussion

This study identifies that colonic enterocytes express a basolateral $P2Y_6$ receptor linking to a sustained activation of NaCl secretion, which is synergistically mediated by cAMP and $[Ca^{2+}]_i$. Previously, a basolateral $P2Y_1$ receptor mediating transient NaCl secretion was identified in rat colon (6). We now show UDP-stimulated NaCl secretion in the rat colon. Since UDP is well known as specific agonist of $P2Y_6$ receptors (1), we assumed that rat colonic mucosa also expresses this receptor. This is proven by a number of independent arguments: (a) UDP-induced small $[Ca^{2+}]_i$ elevation in colonic crypts; (b) identification of $P2Y_6$ receptor mRNA from colonic crypts; and (c) immunohistochemistry showing mucosal expression of $P2Y_6$ receptors in colonic enterocytes. Thus, like other epithelial tissues, multiple different P2 receptors are expressed in the same tissue (2, 7).

In addition to these novel results, we noticed an intriguing difference between the ATP- and the UDP-stimulated NaCl secretory responses. As elaborated in an earlier study, $P2Y_1$ receptor stimulation resulted in a transient NaCl secretory response with typical rank order of potency of nucleotides (2Me-S-ATP > ADP > ATP) (6). The $P2Y_1$-mediated secretion was not influenced by 293B. The isolated colonic crypt $[Ca^{2+}]_i$ signal shows close temporal correlation with the secretory response, and we showed that $P2Y_1$ receptor stimulation only transiently activates basolateral SK4 channels to augment the driving force for luminal Cl^- exit (our unpublished observation).

In sharp contrast, the UDP-stimulated secretion was always sustained, suggesting a different mechanism of activation. Intriguingly, the UDP-stimulated secretion could be completely inhibited with 293B. This compound specifically inhibits the basolateral cAMP-activated KCNQ1/KCNE3 K^+ channel resulting in a complete block of Cl^- secretion in the colon (14, 19). In contrast to KCNQ1 channels in other epithelia in the colon, there is no evidence for Ca^{2+}-mediated regulation of KCNQ1/KCNE3 (19). Thus, these results suggest that activation of colonic $P2Y_6$ receptors elevate cytosolic cAMP and $[Ca^{2+}]_i$ to activate secretion, whereas ATP-induced $P2Y_1$ receptor activation stimulates $[Ca^{2+}]_i$-mediated secretion. This hypothesis is strengthened by the results showing that similar to PGE_2, UDP also increased cAMP in colonic crypts, whereas ATP did not. Nucleotide-mediated stimula-

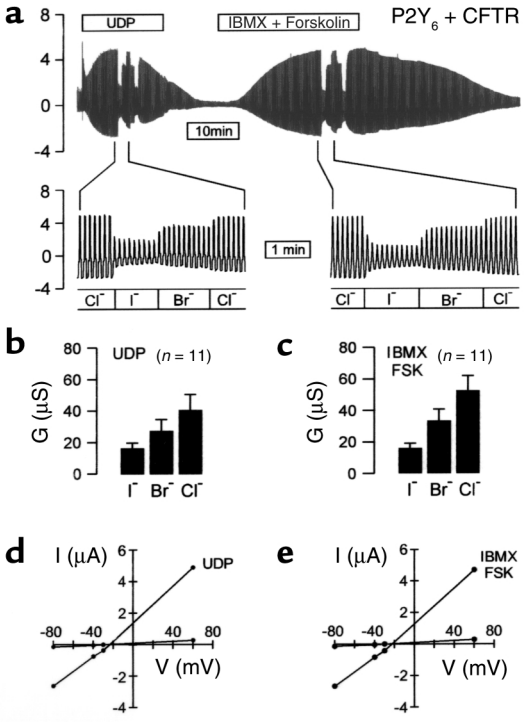

Figure 7
Effect of UDP and IBMX + forskolin on whole-cell conductance in oocytes expressing the $P2Y_6$ receptor and CFTR (UDP 10 μM, IBMX 1 mM, forskolin 2 μM). (**a**) Original recording of a typical experiment. Application of UDP led to a fast and transient conductance increase followed by a slower increase resembling the effect induced by IBMX + forskolin. (**b**) Summary of the halide conductance sequence experiments with UDP and (**c**) IBMX + forskolin. (**d**) Current-voltage relationship of the UDP-induced and the (**e**) IBMX + forskolin-induced conductance. Note the similarity of the halide conductance sequence and the current-voltage relationship of UDP-treated and IBMX + forskolin–treated oocytes.

tion of secretion in airway epithelium has been shown to occur indirectly by Ca^{2+}-dependent autogeneration and paracrine generation of prostanoids (26). We therefore investigated the UDP-mediated NaCl secretion also in the presence of indomethacin. Since 70% of the UDP effect was inhibited with supramaximal concentrations of indomethacin, our results support the finding of nucleotide receptor–mediated release of prostaglandins. PGE_2 is well established as potent secretory agonist in colonic tissue (10). Thus, a large part of the UDP-mediated stimulation of Cl^- secretion apparently occurs through the generation of prostaglandins and a subsequent stimulation of an epithelial cAMP increase. In analogy to other epithelial organs where prostaglandin release was shown to originate form epithelial cells, we suggest that a similar phenomenon is true in colonic mucosa (26, 30). Our results, however, do not rule out whether, in addition to a "direct" epithelial effects, other subepithelial cells (e.g., immunocytes) contribute in an "indirect" way to the observed UDP-stimulated secretion. In fact, a UDP-mediated subepithelial generation of prostaglandins may be expected because the subepithelial layer has been shown to be the predominant location for, for example, bradykinin-stimulated PGE_2 release (31). Thus the P2Y6 receptor may well be expressed in rat colonic submucosa.

A significant fraction of the UDP-mediated NaCl secretory response, however, remained in the presence of indomethacin. We therefore speculated that UDP could lead to an elevation of cAMP, independent of the effect of prostaglandins.

We chose the *Xenopus* oocyte expression system to investigate the signal transduction further, since these cells neither express P2 nor prostanoid receptors. Expectedly, heterologous expression of the receptors in *Xenopus* oocytes revealed that both receptors couple to phospholipase C and subsequently increase $[Ca^{2+}]_i$ (32). To test our hypothesis that the $P2Y_6$ receptor could elevate cAMP we coexpressed the $P2Y_1$ or $P2Y_6$ receptor together with the cAMP-regulated CFTR Cl^- channel. A two-electrode voltage clamp was used to monitor nucleotide-induced oocyte Cl^- currents. We found that in $P2Y_1$ receptor–expressing oocytes ATP transiently activated the endogenous Ca^{2+}-activated Cl^- current, but not the CFTR Cl^- current. In contrast in $P2Y_6$ receptor–expressing oocytes, UDP transiently activated the endogenous Ca^{2+}-activated Cl^- current and, subsequently, CFTR. CFTR Cl^- currents were identified by their characteristic halide conductance sequence ($Cl^->Br^->I^-$). They could unequivocally be differentiated at 6 minutes after UDP stimulation because at that time the Ca^{2+}-activated endogenous Cl^- current had already returned to near resting values (see Figures 4b and 5e). Thus, in addition to the known coupling of the $P2Y_6$ receptor to $[Ca^{2+}]_i$, we report that stimulation of this receptor activates CFTR in *Xenopus* oocytes.

Taken together, we provide evidence from two experimental preparations indicating that stimulation of the $P2Y_6$ receptor leads to the activation of cAMP-regulated ion channels, namely KCNQ1/KCNE3 in colonic mucosa and CFTR in *Xenopus* oocytes.

Intriguingly, activation of the $P2Y_1$ receptors in the same tissues did not stimulate either of the channels. Thus, these data suggest that $P2Y_6$ receptor stimulation differentially elicits an elevation of cAMP in both preparations. The mechanism of this $P2Y_6$ receptor-mediated cAMP elevation remains uncertain and requires further studies. A direct dual coupling to $G_{\alpha q}$ and $G_{\alpha s}$ was recently reported for the $P2Y_{11}$ receptor expressed in CHO-K1 cells (33), but could not be shown in cells expressing the $P2Y_6$ receptor (22). Besides a direct coupling to $G_{\alpha s}$, other signaling events could lead to an increase of cAMP. These include a cAMP increase secondary to a $[Ca^{2+}]_i$-mediated inhibition of a phosphodiesterase or a $[Ca^{2+}]_i$/PKC-mediated activation of adenylyl cyclase(34, 35). In *Xenopus* oocytes CFTR activation by $P2Y_6$ receptor stimulation indicates an elevation of cAMP. Attempts to directly measure oocyte cAMP using the above-mentioned technique and a dye-based approach (FICRhR; Molecular Probes Inc.) were unsuccessful. It must be considered whether CFTR activation by $P2Y_6$ receptors could also have occurred by activation of PKC, which is described as prerequisite for a cAMP-mediated activation of CFTR (36).

An interesting pathophysiological issue has been discovered recently for $P2Y_6$ receptors. $P2Y_6$ receptors are significantly upregulated in T cells infiltrating regions of inflamed bowel and are involved in monocytic release of IL-8 (36–38). Thus, their role in innate immune defense reactions is apparent, and this may well also involve the epithelial sheet of the bowel wall. It is well established that immunocytes are a source of nucleotide release (2). It is thus speculated that $P2Y_6$ receptors are involved in diarrhea of inflammatory bowel disease.

In summary, we describe the expression of a basolateral $P2Y_6$ receptor in rat colonic enterocytes. Activation of this receptor stimulates a sustained NaCl secretion via a synergistic increase of $[Ca^{2+}]_i$ and cAMP.

Acknowledgments

We gratefully acknowledge the expert technical assistance of Helga Schauer, Anna Hopf, and Gerlinde Kummer. Supported by Deutsche Forschungsgemeinschaft Le 942/4-1 and the Danish Medical Research Council.

1. Communi, D., and Boeynaems, J.M. 1997. Receptors responsive to extracellular pyrimidine nucleotides. *Trends Pharmacol. Sci.* **18**:83–86.
2. Ralevic, V., and Burnstock, G. 1998. Receptors for purines and pyrimidines. *Pharmacol. Rev.* **50**:413–492.
3. Hollopeter, G., et al. 2001. Identification of the platelet ADP receptor targeted by antithrombotic drugs. *Nature.* **409**:202–207.
4. Zhang, F.L. 2002. P2Y(13): identification and characterization of a novel Galphai-coupled ADP receptor from human and mouse. *J. Pharmacol. Exp. Ther.* **301**:705–713.
5. Mason, S.J., Paradiso, A.M., and Boucher, R.C. 1991. Regulation of transepithelial ion transport and intracellular calcium by extracellular ATP in human normal and cystic fibrosis airway epithelium. *Br. J. Pharmacol.* **103**:1649–1656.
6. Leipziger, J., Kerstan, D., Nitschke, R., and Greger, R. 1997. ATP increases $[Ca^{2+}]_i$ and ion secretion via a basolateral P2Y receptor in rat distal colonic mucosa. *Pflügers Arch.* **434**:77–83.
7. Hwang, T.H., Schwiebert, E.M., and Guggino, W.B. 1996. Apical and

basolateral ATP stimulates tracheal epithelial chloride secretion via multiple purinergic receptors. *Am. J. Physiol.* **270**:C1611–C1623.
8. Cressman, V.L., et al. 1999. Effect of loss of $P2Y_2$ receptor gene expression on nucleotide regulation of murine epithelial Cl^- transport. *J. Biol. Chem.* **274**:26461–26468.
9. Kunzelmann, K., and Mall, M. 2002. Electrolyte transport in the Mammalian colon: mechanisms and implications for disease. *Physiol. Rev.* **82**:245–289.
10. Binder, H.J., and Sandle, G.I. 1994. Electrolyte transport in the mammalian colon. In Physiology of the gastrointestinal tract. L.R. Johnson, editor. Raven Press. New York, New York, USA. 2133–2171.
11. Greger, R., et al. 1997. Regulation of ion transport in colonic crypts. *News Physiol. Sci.* **12**:62–66.
12. Greger, R. 2000. Role of CFTR in the colon. *Annu. Rev. Physiol.* **62**:467–491.
13. Warth, R., and Bleich, M. 2000. K^+ channels and colonic function. *Rev. Physiol. Biochem. Pharmacol.* **140**:1–62.
14. Schroeder, B.C. 2000. A constitutively open potassium channel formed by KCNQ1 and KCNE3. *Nature.* **403**:196–199.
15. Bleich, M., et al. 1996. Ca^{2+} regulated K^+ and non-selective cation channels in the basolateral membrane of rat colonic crypt base cells. *Pflügers Arch.* **432**:1011–1022.
16. Cartwright, C.A., McRoberts, J.A., Mandel, K.G., and Dharmsathaphorn, K. 1985. Synergistic action of cyclic adenosine monophosphate- and calcium-mediated chloride secretion in a colonic epithelial cell line. *J. Clin. Invest.* **76**:1837–1842.
17. Kerstan, D., Gordjani, N., Nitschke, R., Greger, R., and Leipziger, J. 1998. Luminal ATP induces K^+ secretion via a $P2Y_2$ receptor in rat distal colonic mucosa. *Pflügers Arch.* **436**:712–716.
18. Lehrmann, H., Wittekindt, O., and Leipziger, J. 2002. Luminal $P2Y_2$ receptor-mediated inhibition of electrogenic Na^+ absorption in mouse distal colon. *Pflügers Arch.* **443**:S358 (Abstr.)
19. Lohrmann, E., et al. 1995. A new class of inhibitors of cAMP-mediated Cl^- secretion in rabbit colon, acting by the reduction of cAMP-activated K^+ conductance. *Pflügers Arch.* **429**:S17–530.
20. Siemer, C., and Gögelein, H. 1993. Effects of forskolin on crypt cells of rat distal colon activation of nonselective cation channels in the crypt base and a chloride conductance pathway in other parts of the crypt. *Pflügers Arch.* **424**:321–328.
21. Tokuyama, Y., Hara, M., Jones, E.M.C., and Fan, Z.B.G.I. 1995. Cloning of rat and mouse P2Y purinoceptors. *Biochem. Biophys. Res. Commun.* **211**:211–218.
22. Chang, K., Hanaoka, K., Kumada, M., and Takuwa, Y. 1995. Molecular cloning and functional analysis of a novel P2 nucleotide receptor. *J. Biol. Chem.* **270**:26152–26158.
23. Leipziger, J., et al. 2000. PKA site mutations of ROMK2 channels shift the pH dependence to more alkaline values. *Am. J. Physiol. Renal Physiol.* **279**:F919–F926.
24. Nichols, R.A., Watt, W.C., Lazarowski, E.R., and Harden, T.K. 1996. Uridine nucleotide selectivity of three phospholipase C-activating P2 receptors: identification of a UDP-selective, a UTP-selective, and an ATP- and UTP-specific receptor. *Mol. Pharmacol.* **50**:224–229.
25. Suessbrich, H., et al. 1996. Specific blockade of slowly activation I_{sK} channels by chromanols-impact on the role of I_{sK} channels in epithelia. *FEBS Lett.* **396**:271–275.
26. Lazarowski, E.R., Boucher, R.C., and Harden, T.K. 1994. Calcium-dependent release of arachidonic acid in response to purinergic receptor activation in airway epithelium. *Am. J. Physiol.* **266**:C406–C415.
27. Hardcastle, J., and Hardcastle, P.E.T. 1988. Involvement of prostaglandins in histamin-induced fluid and electrolyte secretion by rat colon. *J. Pharm. Pharmacol.* **40**:106–110.
28. Diener, M., Bridges, R.J., Knobloch, S.F., and Rummel, W. 1988. Neuronally mediated and direct effects of prostaglandins on ion transport in rat colon descendens. *Naunyn Schmiedebergs Arch. Pharmacol.* **337**:74–78.
29. Bailey, M.A., et al. 2001. Evidence for basolateral P2Y(6) receptors along the rat proximal tubule: functional and molecular characterization. *J. Am. Soc. Nephrol.* **12**:1640–1647.
30. Cheuk, B.L., Ko, W.H., and Wong, P.Y. 2002. COX-dependent and -independent pathways in bradykinin-induced anion secretion in rat epididymis. *J. Cell Physiol.* **191**:217–226.
31. Lawson, L.D., and Powell, D.W. 1987. Bradykinin-stimulated eicosanoid synthesis and secretion by rabbit ileal components. *Am. J. Physiol.* **252**:G783–G790.
32. von Küglegen, I., and Wetter, A. 2000. Molecular pharmacology of P2Y-receptors. *Naunyn Schmiedebergs. Arch. Pharmacol.* **362**:310–323.
33. Communi, D., Govaerts, C., Parmentier, M., and Boeynaems, J.M. 1997. Cloning of a human purinergic P2Y receptor coupled to phospholipase C and adenylyl cyclase. *J. Biol. Chem.* **272**:31969–31973.
34. Warhurst, G., Fogg, K.E., Higgs, N.B., Tonge, A., and Grundy, J. 1994. Ca^{2+}-mobilizing agonists potentiate forskolin- and VIP-stimulated cAMP production in human colonic cell line, HT29-cl.19A: role of $[Ca^{2+}]_i$ and protein kinase C. *Cell Calcium*. **15**:162–174.
35. Cooper, D.M., Mons, N., and Karpen, J.W. 1995. Adenylyl cyclases and the interaction between calcium and cAMP signaling. *Nature.* **374**:421–424.
36. Jia, Y., Mathews, C.J., and Hanrahan, J.W. 1997. Phosphorylation by protein kinase C is required for acute activation of cystic fibrosis transmembrane conductance regulator by protein kinase A. *J. Biol. Chem.* **272**:4978–4984.
37. Somers, G.R., Hammet, F.M., Trute, L., Southey, M.C., and Venter, D.J. 1998. Expression of the P2Y6 purinergic receptor in human T cells infiltrating inflammatory bowel disease. *Lab. Invest.* **78**:1375–1383.
38. Warny, M., et al. 2001. P2Y6 nucleotide receptor mediates monocyte interleukin-8 production in response to UDP or lipopolysaccharide. *J. Biol. Chem.* **276**:26051–26056.